Chromatin structure and its chemical modifications regulate the ubiquitin ligase substrate selectivity of UHRF1

Robert M. Vaughan[a], Bradley M. Dickson[a], Matthew F. Whelihan[b], Andrea L. Johnstone[b], Evan M. Cornett[a], Marcus A. Cheek[b], Christine A. Ausherman[a], Martis W. Cowles[b], Zu-Wen Sun[b], and Scott B. Rothbart[a,1]

[a]Center for Epigenetics, Van Andel Research Institute, Grand Rapids, MI 49503; and [b]EpiCypher, Inc., Research Triangle Park, NC 27713

Edited by Steven E. Jacobsen, University of California, Los Angeles, CA, and approved July 25, 2018 (received for review April 12, 2018)

Mitotic inheritance of DNA methylation patterns is facilitated by UHRF1, a DNA- and histone-binding E3 ubiquitin ligase that helps recruit the maintenance DNA methyltransferase DNMT1 to replicating chromatin. The DNA methylation maintenance function of UHRF1 is dependent on its ability to bind chromatin, where it facilitates monoubiquitination of histone H3 at lysines 18 and 23, a docking site for DNMT1. Because of technical limitations, this model of UHRF1-dependent DNA methylation inheritance has been constructed largely based on genetics and biochemical observations querying methylated DNA oligonucleotides, synthetic histone peptides, and heterogeneous chromatin extracted from cells. Here, we construct semisynthetic mononucleosomes harboring defined histone and DNA modifications and perform rigorous analysis of UHRF1 binding and enzymatic activity with these reagents. We show that multivalent engagement of nucleosomal linker DNA and dimethylated lysine 9 on histone H3 directs UHRF1 ubiquitin ligase activity toward histone substrates. Notably, we reveal a molecular switch, stimulated by recognition of hemimethylated DNA, which redirects UHRF1 ubiquitin ligase activity away from histones in favor of robust autoubiquitination. Our studies support a noncompetitive model for UHRF1 and DNMT1 chromatin recruitment to replicating chromatin and define a role for hemimethylated linker DNA as a regulator of UHRF1 ubiquitin ligase substrate selectivity.

epigenetics | DNA methylation | histone posttranslational modifications | nucleosomes | E3 ligase

DNA methylation is a key epigenetic regulator of chromatin-templated biological processes, and aberrant DNA methylation patterning is a hallmark of human cancer and other diseases (1, 2). Found predominantly at CpG dinucleotides in mammals, 5-methylcytosine exists in hemimethylated (HeDNA) and symmetrically methylated (SyDNA) forms. Patterns of 5-methylcytosine are maintained through cell division largely by the maintenance methyltransferase DNMT1 and the E3 ubiquitin ligase UHRF1 (3–6). The DNA methylation maintenance function of UHRF1 depends on its ability to bind chromatin, where it facilitates H3K18 and H3K23 monoubiquitination, a docking site for DNMT1 (7–11).

The interconnected activities of the UHRF1 writer and reader domains (Fig. 1*A*) have been the subject of recent biochemical and genetic studies (10, 12, 13). However, biochemical characterization of UHRF1 regulatory functions, and in particular the mechanisms of interdomain crosstalk through multivalency and allostery, have relied largely on studies with modified histone peptides, methylated short DNA oligonucleotides, and heterogeneous chromatin extracts. Here, we construct semisynthetic recombinant mononucleosomes harboring defined DNA and histone modifications (dNucs) and use these more physiologically relevant reagents to scrutinize the influence of chromatin architecture on UHRF1 regulatory function.

Results

Nucleosomal Linker DNA and H3K9me2 Enhance UHRF1 Enzymatic Activity. UHRF1 binds histone H3 through multivalent engagement of H3K9me2/me3 by its linked TTD-PHD (tandem Tudor and plant homeodomain finger) (14). To determine the contribution of H3K9me2 to the enzymatic activity of UHRF1, we used native chemical ligation to attach a synthetic H3K9me2 peptide to N-terminally truncated histone H3 (*SI Appendix*, Fig. S1 *A* and *B*) and wrapped semisynthetic histone octamers with the 601 nucleosome positioning sequence (15) composed of either no linker DNA (147 bp) or an additional 20 base pairs (187 bp) that extend from each end of the 601 nucleosome positioning sequence (*SI Appendix*, Fig. S1 *C*–*E*). Comparing the usage of peptide, octamer, and dNucs as substrates for in vitro ubiquitination reactions with UHRF1, using recombinant enzymatic components (E1, E2, E3, and ubiquitin), dNucs wrapped with 187-bp linker DNA were preferentially ubiquitinated by UHRF1 (Fig. 1*B*). Furthermore, H3K9me2 enhanced the ubiquitin ligase activity of UHRF1 toward this dNuc substrate.

We previously showed that the ubiquitin ligase activity of UHRF1 toward histone peptide substrates was stimulated by free HeDNA oligonucleotides (10). Consistently, free HeDNA stimulated the activity of UHRF1 toward H3K9me2-containing peptides and octamers and toward itself [autoubiquitination (auto-ub)] (Fig. 1*C*). However, the addition of free DNA, regardless of methylation state, inhibited dNuc and HeLa mononucleosome ubiquitination by UHRF1 (Fig. 1 *C* and *D*). To determine whether

Significance

DNA methylation and histone posttranslational modifications are key epigenetic marks that contribute to the fine-tuned regulation of gene expression and other chromatin-templated biological processes. Here, we build artificial chromatin templates and reveal key chromatin structural features and epigenetic marks that coordinately regulate the binding and enzymatic activity of the DNA methylation regulator UHRF1. Studying activities of epigenetic regulators in the context of defined chromatin templates, particularly for multidomain histone and DNA binding proteins such as UHRF1, is critical for understanding molecular mechanisms of epigenetic crosstalk and mechanics regulating epigenetic signaling, and for determining how epigenetic dysregulation contributes to human disease.

Author contributions: R.M.V., B.M.D., M.F.W., A.L.J., E.M.C., C.A.A., and S.B.R. designed research; R.M.V., M.F.W., A.L.J., and C.A.A. performed research; M.F.W., M.A.C., M.W.C., and Z.-W.S. contributed new reagents/analytic tools; R.M.V., B.M.D., A.L.J., E.M.C., M.A.C., M.W.C., Z.-W.S., and S.B.R. analyzed data; and R.M.V. and S.B.R. wrote the paper.

Conflict of interest statement: EpiCypher is a commercial developer/supplier of platforms similar to those used in this study: AlphaScreen (Perkin Elmer) interaction assays (i.e., AlphaNuc) and recombinant semisynthetic nucleosomes (dNucs). S.B.R. has served in a compensated consulting role to EpiCypher.

This article is a PNAS Direct Submission.

[1]To whom correspondence should be addressed. Email: Scott.Rothbart@vai.org.

This article contains supporting information online at www.pnas.org/lookup/suppl/doi:10.1073/pnas.1806373115/-/DCSupplemental.

Published online August 13, 2018.

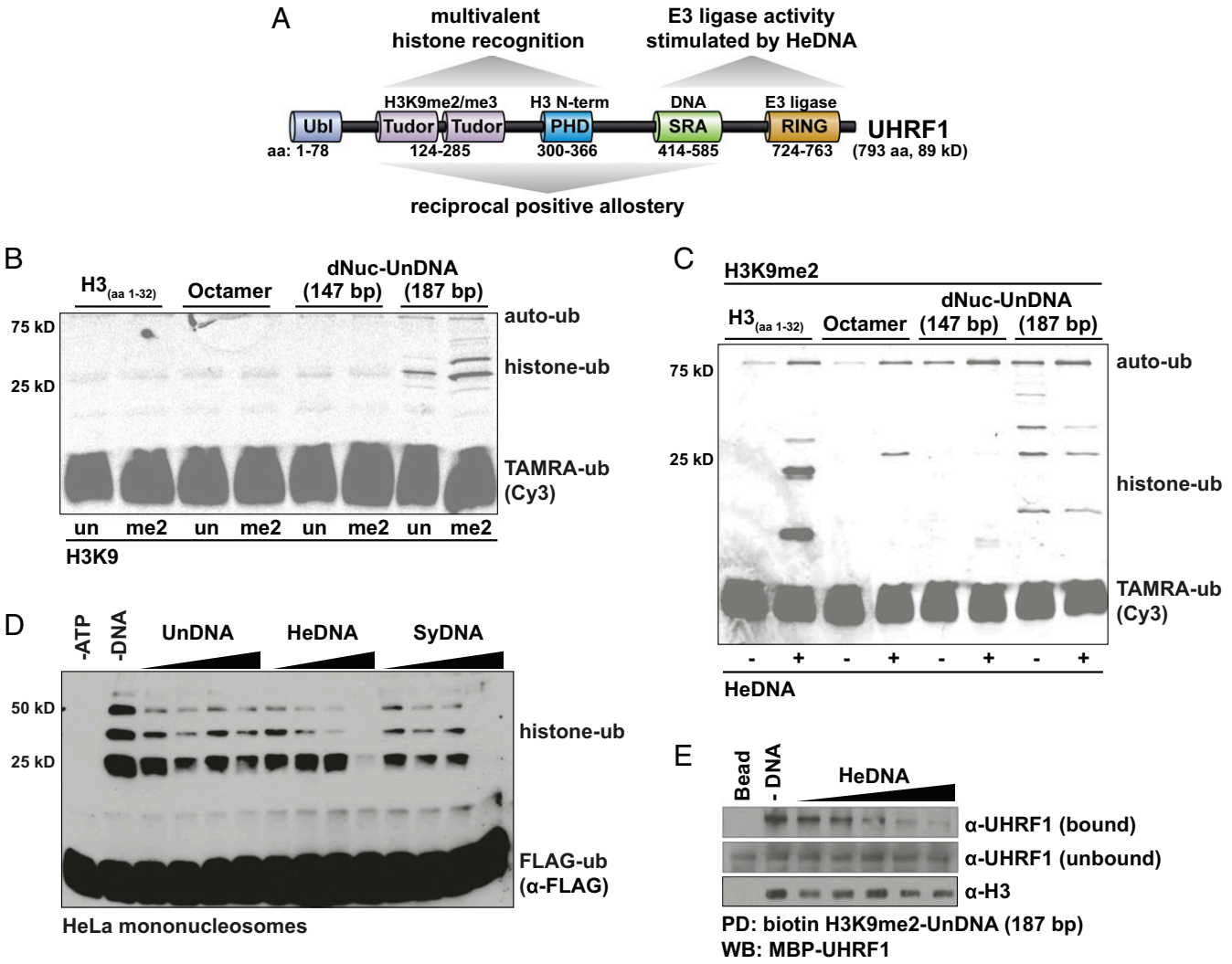

Fig. 1. Linker DNA and H3K9me2 enhance UHRF1 enzymatic activity toward nucleosomal histone substrates. (*A*) Domain map of UHRF1 highlighting known functions and intramolecular crosstalk. Domain boundaries are indicated by amino acid numbering according to Uniprot annotation. (*B*) UHRF1 in vitro ubiquitination reactions with the indicated unmodified (H3K9un) or H3K9me2-containing substrates. dNuc, recombinant designer nucleosomes, wrapped with unmodified DNA (UnDNA). TAMRA-labeled ubiquitin (TAMRA-ub) was imaged in-gel by Cy3 fluorescence. (*C*) UHRF1 in vitro ubiquitination reactions with the indicated substrates in the absence (–) or presence (+) of hemimethylated DNA (HeDNA) oligonucleotides and imaged for TAMRA-ub. (*D*) In vitro ubiquitination of HeLa mononucleosomes by UHRF1 in the absence or presence of increasing concentrations of unmethylated DNA (UnDNA), HeDNA, or symmetrically methylated DNA (SyDNA) oligonucleotides imaged by Western blot for FLAG-ubiquitin. (*E*) Western blot for UHRF1 after pulldown with biotinylated H3K9me2-UnDNA 187-bp dNucs in the absence or presence of increasing concentrations of HeDNA oligonucleotides. Western blots of unbound UHRF1 and H3 are shown for loading controls. All data shown are representative of at least two replicates from independent protein and nucleosome preparations.

free HeDNA inhibited UHRF1 enzymatic activity by blocking nucleosome binding, we performed competitive in vitro nucleosome pulldowns. Indeed, pulldown experiments demonstrated that free HeDNA inhibited the interaction of UHRF1 with dNucs in a concentration-dependent manner (Fig. 1*E*). Collectively, we reveal a key role for linker DNA in the recruitment of UHRF1 to nucleosomes. We further show that both linker DNA and H3K9me2 enhance the enzymatic activity of UHRF1 toward nucleosomal histone substrates. Notably, the presence of linker DNA also promoted UHRF1 auto-ub, suggesting that the combination of histone- and DNA-binding promotes an E3-ligase competent UHRF1 conformation. The UHRF1 interdomain architecture, or supertertiary structure (16), is likely influenced by nucleosome recognition.

Hemimethylated Linker DNA Redirects UHRF1 Enzymatic Activity. As it was previously reported that linker HeDNA enhances UHRF1 interaction with nucleosomes (13), and our studies here demonstrate linker DNA as a requisite for UHRF1 E3 ligase activity, we next sought to clarify the contribution of nucleosomal linker DNA methylation to UHRF1 function. Octamers assembled with either unmodified H3 or H3K9me2 were wrapped with 187 bp of unmodified DNA (UnDNA) or with 187 bp of DNA in which three CpG sites in the 20-base pair linker extensions from the 601 nucleosome positioning sequence were methylated on one (HeDNA) or both (SyDNA) strands (*SI Appendix*, Fig. S1 *C–E*). The 5′ ends of these DNA sequences were functionalized with biotin and a triethyleneglycol spacer to enable binding measurements by an AlphaScreen proximity assay (Fig. 2*A* and *SI Appendix*, Fig. S1 *C–E*). In this assay, biotinylated dNucs are conjugated to streptavidin donor beads, and His-MBP-UHRF1 is conjugated to nickel acceptor beads. The interaction of UHRF1 with the nucleosome brings donor and acceptor beads in proximity. Excitation of donor beads at 680 nm produces singlet oxygen molecules that interact with

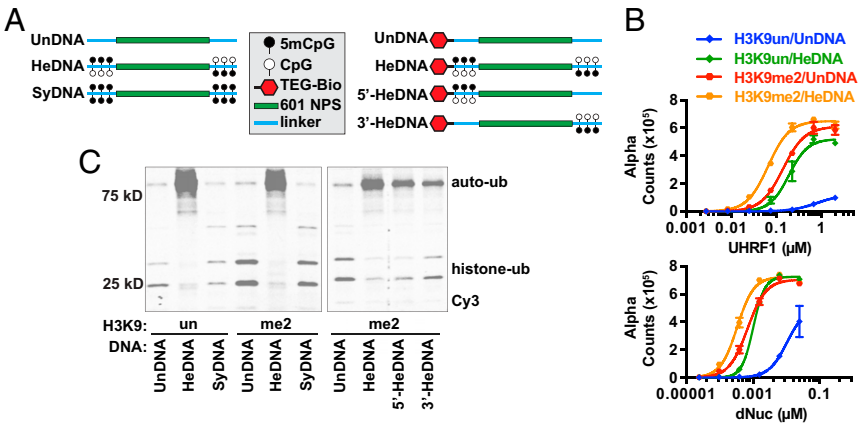

Fig. 2. Hemimethylated linker DNA stimulates UHRF1 autoubiquitination while restricting histone ubiquitination. (*A*) Schematic of methylated linker DNA templates constructed for dNuc reconstitutions. (*B*) AlphaScreen proximity assays with His-MBP-UHRF1 and the indicated biotinylated rNucs. Data shown are representative of two replicates. Error bars ± SEM from technical triplicate measurements. (*C*) UHRF1 in vitro ubiquitination reactions with 187-bp dNuc substrates (H3K9un and H3K9me2 wrapped with the indicated DNA from *A*) imaged in-gel for TAMRA-ub. Data shown are representative of two replicates.

acceptor beads to produce light emission that is captured at 615 nm (*SI Appendix*, Fig. S2*A*).

Consistent with previous measurements with peptides and DNA oligonucleotides (10, 17–21), both H3K9me2 and HeDNA, individually and in combination, enhanced UHRF1 interaction with dNucs (Fig. 2*B* and *SI Appendix*, Fig. S2*B*). However, unlike activity measurements with peptide substrates and free HeDNA (Fig. 1*C*), linker HeDNA (but not UnDNA or SyDNA) restricted UHRF1 enzymatic activity toward nucleosomal histones in favor of robust auto-ub (Fig. 2*C* and *SI Appendix*, Fig. S3 *A* and *B*). As others previously reported the importance of HeDNA positioning within nucleosomal DNA for UHRF1 interaction (13), we evaluated whether HeDNA placement at the 5′ or 3′ end of DNA (Fig. 2*A*) affected the enzymatic activity of UHRF1 (Fig. 2*C*). Both 5′- and 3′-HeDNA wrapped dNucs enhanced UHRF1 auto-ub relative to UnDNA and notably showed roughly half of the UHRF1 auto-ub as HeDNA templates with methylation at both termini. These studies demonstrate a key role for linker HeDNA as an epigenetic regulator of UHRF1 substrate selectivity and suggest auto-ub UHRF1 is uncoupled from DNMT1-mediated DNA methylation control through restriction of its histone ubiquitination activity.

UHRF1 E3 Ligase Substrate Selectivity Is Mediated Through Multivalent DNA and Histone Binding. To further our understanding of how both histone and DNA engagement contribute to the allosteric control of UHRF1 enzymatic activity, we next queried the effect of point mutations known to disrupt key functions of the UHRF1 histone- and DNA-binding domains (*SI Appendix*, Fig. S4). We and others show that point mutations in the UHRF1 PHD (PHD*, D334A/E335A) block the interaction of UHRF1 with the N terminus of H3 by disrupting coordination of the guanidinium group of H3R2 (22–25). UHRF1 PHD* disrupted the enhanced interaction measured by AlphaScreen between UHRF1 and H3K9me2 dNucs (Fig. 3*A*). Notably, PHD* also perturbed the interaction with HeDNA dNucs (both H3K9un and H3K9me2), suggesting a mechanism of allosteric binding, as was previously reported with histone peptides and DNA oligonucleotide binding (10, 12, 26). A point mutation in the SET- and RING-associated (SRA) domain of UHRF1 (SRA*, G448D) disrupts DNA binding by substituting an acidic residue in the DNA binding pocket that repels the negative charge on the phosphate backbone of DNA (10, 18). Consistent with the identified requirement for linker DNA (Fig. 1 *B*–*E*), UHRF1 SRA* resulted in a HeDNA-dependent reduction in dNuc interaction to levels measured through H3K9me2 binding alone (Fig. 3*A*).

We next performed in vitro ubiquitination reactions with WT, PHD*, and SRA* UHRF1, using H3K9me2 dNucs wrapped with HeDNA at the 3′ end (Fig. 3*B*). UHRF1 SRA* had a marked reduction in enzymatic activity toward itself and toward histones. In addition, UHRF1 PHD* abolished histone ubiquitination, consistent with a role for the TTD-PHD as the histone substrate binding module. Notably, HeDNA-dependent auto-ub was also compromised when UHRF1 was unable to engage dNucs through H3 tail recognition (Fig. 3). Collectively, these data show that allosteric control of UHRF1 enzymatic activity is regulated by multivalent nucleosome engagement, and that the competent E3 ligase conformation of UHRF1 requires *cis* intranucleosomal interaction through recognition of the H3 N-terminal tail and

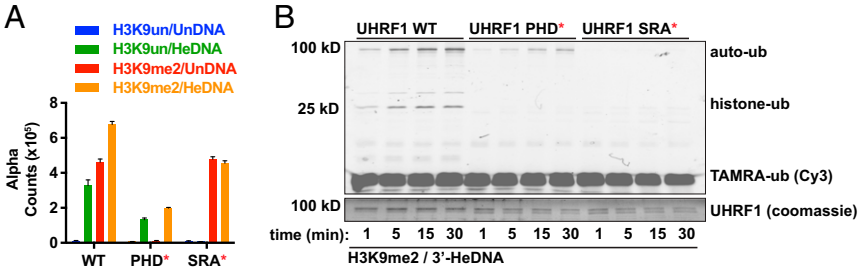

Fig. 3. Allosteric control of UHRF1 E3 ligase activity is regulated by multivalent nucleosome engagement. (*A*) AlphaScreen proximity assays with wild-type (WT) or mutant His-MBP-UHRF1 and the indicated biotinylated dNucs. Data shown are representative of two replicates. Error bars ± SEM from technical triplicate measurements. (*B*) WT and mutant UHRF1 in vitro ubiquitination reactions with H3K9me2/3′-HeDNA dNuc substrates. Data shown are representative of three replicates.

linker DNA (27). Furthermore, our data suggest that the UHRF1–nucleosome interactions are driven largely by histone binding, whereas enzymatic activities of UHRF1 are controlled by the presence and methyl state of nucleosomal DNA.

Functional UHRF1 SRA Domain Promotes DNMT1 Interaction with Nucleosomes. We next sought to determine how the interaction of DNMT1 with nucleosomes was influenced by UHRF1 and its ubiquitin ligase activity. We first performed in vitro ubiquitination reactions with or without biotinylated H3K9me2 dNucs wrapped with unmodified 187 bp DNA in the absence or presence of WT or SRA* UHRF1 (Fig. 4*A*, *Bottom* and *SI Appendix*, Fig. S3*C*). Ubiquitination reactions were quenched and biotinylated nucleosomes were bound to streptavidin magnetic beads. After washing away unbound reaction components, a saturating concentration of recombinant DNMT1 was added to the nucleosome-bead matrix. Consistent with the identified role for the UHRF1 SRA in the interaction with nucleosomes (Fig. 3*A*), Western blots of bound proteins revealed that more WT UHRF1 pulled down in these reactions than SRA* (Fig. 4*A*, *Top*). Notably, WT, but not SRA*, UHRF1 enhanced the interaction of DNMT1 with nucleosomes (Fig. 4*A*). The reciprocal experiment was also performed, in which we pulled down ubiquitinated nucleosomes by MBP-tagged DNMT1 (*SI Appendix*, Fig. S3*D*). Consistently, after in vitro ubiquitination of nucleosomes by UHRF1, more H3 was bound to DNMT1, and this was dependent on the SRA domain of UHRF1. As only a small fraction of H3 was ubiquitinated in these reactions (as indicated by H3K9me2 Western blots), we cannot definitively conclude that binding of DNMT1 to nucleosomes occurs in a H3-ub-dependent manner. However, these experiments demonstrate a critical role for UHRF1 and its interaction with DNA in the recruitment of DNMT1 to nucleosomes.

Discussion

Through systematic evaluation of UHRF1 enzymatic activity on progressively more complex chromatin surrogates, we identified nucleosomal linker DNA and H3K9me2 as requisites for UHRF1-dependent ubiquitination of histone proteins. Ubiquitinated products were consistent in size with mono- and di-ubiquitinated H3, a suggested docking site for DNMT1 (9, 11). Western blots

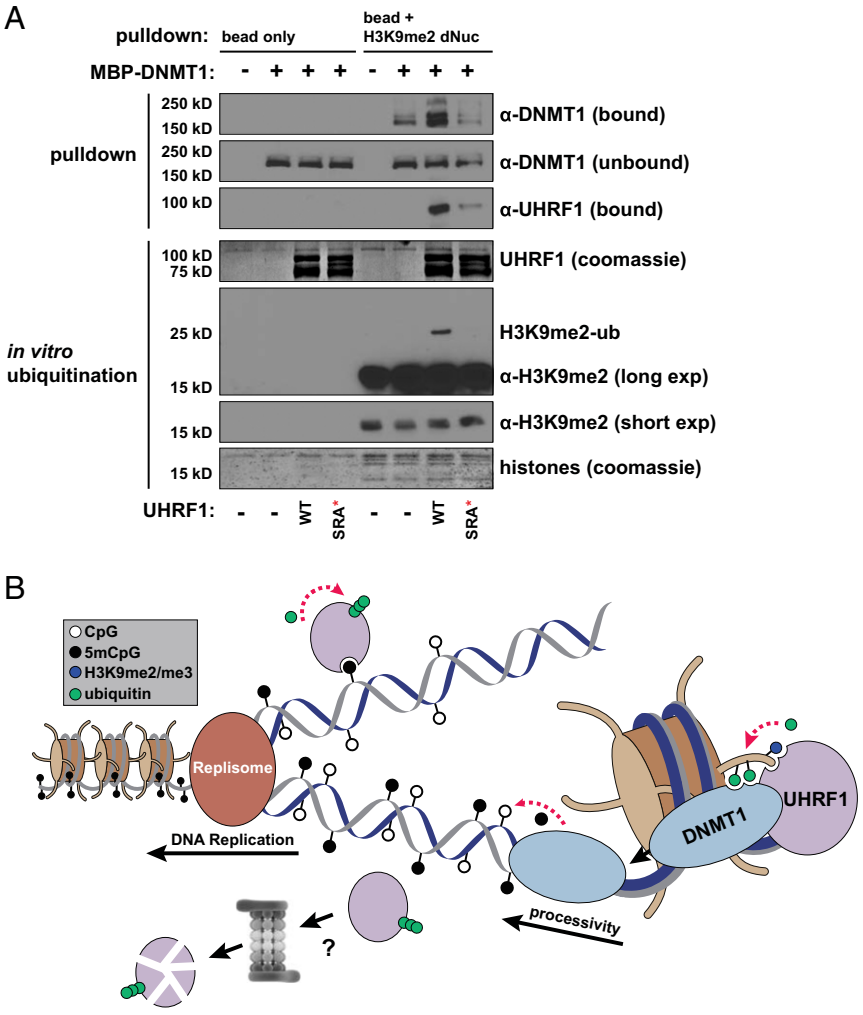

Fig. 4. UHRF1 promotes the binding of DNMT1 to nucleosomes. (*A*) Western blots or Coomassie stains (where indicated) for the indicated proteins after in vitro pulldown assays (*Top*) with biotinylated H3K9me2/187 bp UnDNA nucleosomes or beads that were first used as substrates for in vitro ubiquitination reactions (*Bottom*) with or without UHRF1. Results were confirmed by reciprocal pulldown experiments shown in *SI Appendix*, Fig. S3*D*. (*B*) Model for UHRF1-dependent recruitment of DNMT1 to replicating chromatin. UHRF1 is recruited to nucleosomes marked by H3K9 methylation and unmethylated DNA, where it ubiquitinates H3, a docking site for DNMT1. Through its processive activity and its affinity for hemimethylated DNA, DNMT1 catalyzes methyl transfer at nearby hemimethylated CpG sites. When UHRF1 binds hemimethylated DNA, it autoubiquitinates itself in favor of H3 ubiquitination, making it non-productive as a cofactor for DNA methylation maintenance.

with an H3K9me2 antibody show this histone is marked with ubiquitin at the size corresponding with the major ubiquitin product in these reactions (Fig. 4*A* and *SI Appendix*, Fig. S3*C*), consistent with H3K18ub or H3K23ub being reported by us and others as major sites of UHRF1 enzymatic activity toward nucleosomes (8–10). In addition, we showed that linker HeDNA functioned as an epigenetic switch to modulate the substrate selectivity of UHRF1 toward itself at the expense of histone ubiquitination. Unmethylated linker DNA directs UHRF1 E3 ligase activity toward histone substrates, whereas hemimethylated linker DNA restricts H3 ubiquitination in favor of UHRF1 auto-ub. Consistently, this antagonistic relationship between DNA methylation and UHRF1-dependent histone ubiquitination has been observed, but not explained, after genetic knockdown of DNMT1 (8, 9, 28, 29).

Observation of this mechanism was not possible using histone peptides and DNA oligonucleotides. We add to the growing body of literature, using nucleosomes as templates for chromatin biochemistry (30–33) and caution against the exclusive use of peptide and oligonucleotide reagents to study mechanisms of chromatin regulation.

Our studies expand the current model of UHRF1-directed DNA methylation maintenance, which posits histone ubiquitination as a recruitment mechanism for DNMT1 (8, 9, 11, 30). As DNMT1, UHRF1, and several H3K9 methyltransferases are enriched by nascent chromatin capture (34), we suggest DNMT1 recruitment through UHRF1-dependent H3 ubiquitination occurs in the wake of replicating DNA polymerase at H3K9me2/me3-marked nucleosomes adjacent to regions of HeDNA (Fig. 4*B*). This serves as a nucleation event to bring DNMT1 in proximity to sites of newly replicated DNA. This nucleation model is consistent with the appreciated processive property of DNMT1 enzyme activity (35).

We propose that HeDNA acts as a kinetic trap for UHRF1 and promotes its E3 ligase activity, regardless of the availability of histone substrates. As DNMT1 preferentially modifies HeDNA (36), we suggest HeDNA-induced auto-ub serves as a mechanism to clear UHRF1 from substrates of DNMT1 activity. Consistent with a model in which ubiquitinated UHRF1 is cleared by the proteasome, UHRF1 protein levels increase after proteasome inhibition by MG132 (37, 38). Productive histone ubiquitination by UHRF1 is likely balanced by the activity of a deubiquitinase. As such, dynamic control of UHRF1 auto-ub may add an additional regulatory layer to the replication-coupled inheritance of DNA methylation patterns.

An alternative and intriguing hypothesis generated by our studies and other recent work (39) is that ubiquitinated UHRF1 (or the UBL domain) may serve as a docking site for DNMT1, adding a potential histone-independent recruitment mechanism of DNMT1 to hemimethylated DNA through the SRA domain of UHRF1. Our studies call for rigorous evaluation of the temporal and spatial dynamics of ubiquitin signaling through UHRF1 and its effect on the chromatin targeting and activity of DNMT1.

Materials and Methods

Plasmids and Protein Production. All proteins used in this study align to the major human sequence variants. Full-length UHRF1 was cloned into a modified pQE vector as an N-terminal His-MBP fusion separated by a TEV cleavage site. Mutations (PHD*, D334A/E335A; SRA*, G448D) were introduced by QuikChange site-directed mutagenesis (Agilent). UBA1 was a gift from Cynthia Wolberger (Addgene plasmid #34965). UBCH5A was a gift from Brian Kuhlman. TEV protease was a gift from Jiyan Ma. BL21(DE3) *Escherichia coli* were made chemically competent (Zymo Research), and expression constructs were transformed for 5 min on ice and plated onto prewarmed LB agar plates (ampicillin, 100 μg/mL). Single colonies were picked and grown in LB Lennox (Cassion) with ampicillin (100 μg/mL) at 37 °C until the OD_{600} reached 0.8–1.0. The temperature was then lowered to 16 °C, isopropyl β-D-1-thiogalactopyranoside (RPI) was added to a final concentration of 0.5 mM, and cultures were incubated overnight with shaking. Expression was checked by SDS/PAGE, followed by Coomassie brilliant blue staining. Cells were collected by centrifugation (5,000 × *g*, 10 min, 4 °C), and resuspended in buffer A (50 mM Tris at pH 8.0, 500 mM NaCl, 20 mM imidazole) with 1 mM PMSF and 1 mM DTT. Once resuspended, cells were either frozen at −80 °C or lysed by the addition of lysozyme (1 h on ice), followed by sonication on ice (5 × 20 s, with 2 min rest between cycles). Insoluble material was then cleared by centrifugation (38,000 × *g*, 30 min, 4 °C). His60 Superflow resin (Clontech) was equilibrated in buffer A and was mixed with cleared lysate for 1 h at 4 °C (2.5 mL of resin was used for every 2 L of *E. coli* culture). The resin and bound protein was washed three times with at least 20 bed volumes of buffer A, followed by elution of His-tagged proteins in five bed volumes of buffer B (25 mM Hepes at pH 7.5, 100 mM NaCl, 1 mM DTT). Proteins were concentrated (Amicon Ultra Centrifugal Filters) and further purified by size-exclusion chromatography (25 mM Hepes at pH 7.5, 100 mM NaCl, Superdex 200; GE Healthcare). Fractions were checked for purity by SDS/PAGE, followed by Coomassie blue staining, pooled and concentrated, and frozen with 20% glycerol. Enzyme assays were performed with tagless UHRF1. For cleavage of the His-MBP tag from UHRF1, tagged UHRF1 (>50 μM) was combined with TEV protease (500 nM) in dialysis tubing (SnakeSkin, 7K MWCO), and dialyzed overnight at 4 °C into TEV cleavage buffer (50 mM Tris at pH 8.0, 1 mM DTT, 0.5 mM EDTA). Cleaved UHRF1 was separated from His-MBP by size exclusion, concentrated (>20 μM), and snap frozen.

Recombinant DNMT1 was produced using a baculoviral expression system in Sf9 insect cells and purified by single-step affinity purification. Briefly, full-length DNMT1 was cloned into a modified pFastbac vector fused to an N-terminal 6× histidine and an oxide-dissolving maltose binding protein (HisoMBP), followed by a TEV cleavage site (the modified pFastbac vector was a generous gift from H. Eric Xu). Baculovirus was generated according to the Bac-to-Bac protocol (Invitrogen). After transduction, cells were harvested by centrifugation and resuspended in lysis buffer (50 mM Tris at pH 8.0, 250 mM NaCl, 15 mM imidazole, 5% glycerol, 1 mM DTT, 1 mM PMSF, 0.1% Triton X-100, and one tablet of complete protease inhibitor [Roche] per 20 mL buffer). Cells were kept on ice for 20 min, followed by centrifugation (38,000 × *g*, 30 min, 4 °C). Soluble DNMT1 was affinity purified as described here for purification of UHRF1, without the size exclusion chromatography.

Ubiquitination Assays. Ubiquitination reactions were performed in 20 μL ubiquitin assay buffer (50 mM Hepes at pH 7.5, 66 mM NaCl, 2.5 mM $MgCl_2$, and 2.5 mM DTT) for 20 min at room temperature (RT), unless otherwise indicated for time course reactions (Fig. 3*B*: 1, 5, 15, 30 min; *SI Appendix*, Fig. S3*A*: 1, 3, 5, 15, 30, 60, 90, 120 min). The ubiquitin machinery, including 50 nM E1 (UBA1), 667 nM E2 (UBCH5A), 1.5 μM E3 (UHRF1), and 5 μM ubiquitin (FLAG-ub, BostonBiochem or TAMRA-ub, BioVision), was charged with the addition of ATP (8 mM). Next, 440 nM peptide ($H3_{(1-32)}$K9me2) or 220 nM nucleosomes (HeLa mononucleosomes and dNucs) were added. Where indicated, duplex DNA oligonucleotides were added to the reaction (5′-CCATGXGCTGAC-3′ and 5′-GTCAGYGCATGG-3′; UnDNA: X is cytosine and Y is cytosine; HeDNA: X is 5-methylcytosine and Y is cytosine) at the concentrations listed: Fig. 1*C*, 6.25 μM; Fig. 1*D*, 1, 6, 20, 80 μM. Reactions were quenched by the addition of SDS loading buffer to a final concentration of 1×. Fresh beta-mercaptoethanol was added to the SDS loading buffer to reduce E1-ub and E2-ub conjugates for all reactions. Reactions were separated by SDS/PAGE and either imaged directly by fluorescence detection of TAMRA-ub (Azure c400) or immunoblotted for FLAG-ub. Gel images and blots shown are representative of at least two independent experiments (separate protein preps and nucleosome reconstitutions).

In Vitro Pulldowns. All pulldown assays were performed in pulldown buffer (25 mM Hepes at pH 7.5, 100 mM NaCl, 0.5% BSA, 0.1% Nonidet P-40). For each nucleosome pulldown in Fig. 1*E*, 5 μL streptavidin-coated beads (Pierce) were incubated with 5 pmol recombinant H3K9me2-UnDNA 187-bp biotinylated nucleosomes for 30 min at RT. Beads were washed 2× in pulldown buffer. His-MBP-tagged UHRF1 (1 μM) was incubated with conjugated beads in pulldown buffer (200 μL) overnight at 4 °C in the presence of increasing concentrations (0.5, 1, 10, 50, and 100 μM) of HeDNA (same oligonucleotide as in ubiquitination reaction). Unbound UHRF1 was collected for analysis as an input control. Beads were then washed 3× in pulldown buffer and boiled in 100 μL of 1× SDS loading buffer. For Western blot, 10 μL of bound protein and 2% of the unbound fraction was loaded for input onto SDS/PAGE.

For pulldowns of DNMT1 by ubiquitinated nucleosomes (Fig. 4*A* and *SI Appendix*, Fig. S3*C*), ubiquitination reactions were performed as described here for 30 min at RT with biotinylated H3K9me2/UnDNA 187-bp dNucs (500 nM) as substrates. For each pulldown, a 40-μL ubiquitin reaction was quenched by the addition of 10 mM EDTA, followed by incubation on ice. Six microliters of each reaction were loaded onto 15% SDS/PAGE for analysis by Cy3 (TAMRA-ubiquitin), followed by Coomassie blue staining (UHRF1 and histones). The remaining 34 μL was diluted into 200 μL pulldown buffer and incubated with 5 μL streptavidin magnetic beads for 15 min at RT. The beads were washed 2× in pulldown buffer. Next, oMBP-DNMT1 (0.5 μM) was

incubated with the bound nucleosomes overnight at 4 °C in pulldown buffer (200 μL). The unbound DNMT1 was collected for a loading control. The beads were then washed 3× in pulldown buffer. Bound proteins were eluted by boiling in 60 μL of 1× SDS loading buffer. Ten microliters of bound protein and 5% of the unbound fraction were run on SDS/PAGE for analysis by Western blot. For the pulldown of ubiquitinated nucleosomes by DNMT1 (*SI Appendix*, Fig. S3*D*), 5 pmol of MBP-DNMT1 was bound to 5 μL of anti-MBP magnetic beads (New England BioLabs), and the remainder of the procedure was identical to the previously described pulldown.

Western Blotting. Proteins were separated by SDS/PAGE and transferred to PVDF membrane (Amersham Hybond P), using a semidry transfer apparatus (Hoefer) for 1.5 h at a current of 1 mA/cm^2. Membranes were blocked in blotting buffer (1× PBS at pH 7.6, 0.1% Tween-20, 5% BSA) for 1 h at RT; primary antibodies [anti-FLAG, Sigma 1804, 1:5,000; anti-DNMT1, Abcam 134148, 1:2,000; anti-H3K9me2 (Fig. 4), Abcam 1220, 1:10,000; anti-H3K9me2 (*SI Appendix*, Fig. S1), Abclonal A2359, 1:5,000; anti-H3, EpiCypher 13–0001, 1:25,000; anti-MBP, Abcam 9084, 1:5,000; anti-UHRF1, Cell Signaling Technology 12387, 1:2,000] were diluted in blotting buffer and hybridized overnight at 4 °C. Membranes were washed three times for 5 min in PBS-T. HRP-conjugated secondary antibodies (anti-mouse, GE Life Sciences NA931, 1:5,000; anti-rabbit, GE Life Sciences NA934, 1:10,000) were then hybridized at RT for 1 h in blotting buffer. Membranes were again washed three times for 5 min in PBS-T and reacted with ECL Prime (GE Life Sciences). Blots were exposed to film and developed on a Kodak system. ImageJ was used to quantify the signal from monoub H3 in *SI Appendix*, Fig. S3*A*.

Recombinant Nucleosome Production. For wild-type recombinant nucleosomes, recombinant human histones (H3.1, H4, H2A, and H2B) were expressed, purified, and reconstituted into nucleosomes essentially as described (40). For nucleosomes bearing histones with H3K9me2, recombinant H3K9me2 was produced by native chemical ligation as previously described (41) (see also *SI Appendix*, Fig. S1 *A* and *B*) and assembled into nucleosomes as described earlier. The nucleosome assembly DNA sequence contained the 147-bp 601 nucleosome positioning sequence (15) (601-DNA) flanked by 21 bp linker DNA containing 3 CpG sites (*SI Appendix*, Fig. S1*E*). PCR was used to generate UnDNA and HeDNA templates. For HeDNA, primers with methylated CpGs were used to amplify the 601-DNA, generating one methylated and one unmethylated strand. UnDNA was made as described earlier, using unmethylated primers. As SyDNA was not amenable to PCR-based generation, a primer-based ligation strategy was used. Complementary primers (21 bp) were synthesized with three methylated CpGs and T overhangs. The T overhangs were used for directional ligation to a PCR-amplified 601-DNA. For ligation, 147 bp 601-DNA was treated with non-proofreading Taq DNA polymerase (adds A overhangs to the 3′ strand of blunt-ended fragments) and subsequently ligated to the annealed SyDNA fragments, using a Blunt/TA ligase master mix (NEB M0367S). SyDNA templates were generated to more than 90% purity, as analyzed by gel electrophoresis.

UHRF1 AlphaScreen Assay. His-MBP-UHRF1 and biotinylated dNucs were diluted in 25 mM Hepes at pH 7.5, 250 mM NaCl, and 0.05% Nonidet P-40. UHRF1 (200 nM or titrated where indicated) was incubated with the dNucs (1 nM or titrated where indicated) in 384-well plates (AlphaPlate-384; Perkin-Elmer) for 30 min at RT. Streptavidin Donor Beads (Perkin-Elmer) and Nickel Chelate Acceptor Beads (AlphaScreen Histidine Detection Kit; Perkin-Elmer) were then added to a final concentration of 20 μg/mL After 60 min, Alpha Counts were read using an EnVision Plate Reader (Perkin-Elmer). Data were analyzed in GraphPad Prism, using nonlinear regression analysis for curve fitting. Error bars represent SEM from technical triplicates.

ACKNOWLEDGMENTS. We thank members of the S.B.R. laboratory, Mark Bedford, Patrick Grohar, and Gerd Pfeifer for helpful discussions and insight. We also thank Jonathan Burg for technical assistance with nucleosome preparation and Amy Nelson for administrative support. This work was supported by the Van Andel Research Institute, Van Andel Institute Graduate School, and National Institutes of Health Grants R35GM124736 (to S.B.R.), R43CA212733 (to Z.-W.S.), and R44CA212733 (to Z.-W.S.).

1. Edwards JR, Yarychkivska O, Boulard M, Bestor TH (2017) DNA methylation and DNA methyltransferases. *Epigenetics Chromatin* 10:23.
2. Baylin SB, Jones PA (2016) Epigenetic determinants of cancer. *Cold Spring Harb Perspect Biol* 8:a019505.
3. Li E, Bestor TH, Jaenisch R (1992) Targeted mutation of the DNA methyltransferase gene results in embryonic lethality. *Cell* 69:915–926.
4. Liao J, et al. (2015) Targeted disruption of DNMT1, DNMT3A and DNMT3B in human embryonic stem cells. *Nat Genet* 47:469–478.
5. Sharif J, et al. (2007) The SRA protein Np95 mediates epigenetic inheritance by recruiting Dnmt1 to methylated DNA. *Nature* 450:908–912.
6. Bostick M, et al. (2007) UHRF1 plays a role in maintaining DNA methylation in mammalian cells. *Science* 317:1760–1764.
7. Rothbart SB, et al. (2012) Association of UHRF1 with methylated H3K9 directs the maintenance of DNA methylation. *Nat Struct Mol Biol* 19:1155–1160.
8. Nishiyama A, et al. (2013) Uhrf1-dependent H3K23 ubiquitylation couples maintenance DNA methylation and replication. *Nature* 502:249–253.
9. Qin W, et al. (2015) DNA methylation requires a DNMT1 ubiquitin interacting motif (UIM) and histone ubiquitination. *Cell Res* 25:911–929.
10. Harrison JS, et al. (2016) Hemi-methylated DNA regulates DNA methylation inheritance through allosteric activation of H3 ubiquitylation by UHRF1. *eLife* 5:e17101.
11. Ishiyama S, et al. (2017) Structure of the Dnmt1 reader module complexed with a unique two-mono-ubiquitin mark on histone H3 reveals the basis for DNA methylation maintenance. *Mol Cell* 68:350–360.e7.
12. Fang J, et al. (2016) Hemi-methylated DNA opens a closed conformation of UHRF1 to facilitate its histone recognition. *Nat Commun* 7:11197.
13. Zhao Q, et al. (2016) Dissecting the precise role of H3K9 methylation in crosstalk with DNA maintenance methylation in mammals. *Nat Commun* 7:12464.
14. Arita K, et al. (2012) Recognition of modification status on a histone H3 tail by linked histone reader modules of the epigenetic regulator UHRF1. *Proc Natl Acad Sci USA* 109:12950–12955.
15. Lowary PT, Widom J (1998) New DNA sequence rules for high affinity binding to histone octamer and sequence-directed nucleosome positioning. *J Mol Biol* 276:19–42.
16. Tompa P (2012) On the supertertiary structure of proteins. *Nat Chem Biol* 8:597–600.
17. Karagianni P, Amazit L, Qin J, Wong J (2008) ICBP90, a novel methyl K9 H3 binding protein linking protein ubiquitination with heterochromatin formation. *Mol Cell Biol* 28:705–717.
18. Avvakumov GV, et al. (2008) Structural basis for recognition of hemi-methylated DNA by the SRA domain of human UHRF1. *Nature* 455:822–825.
19. Hashimoto H, et al. (2008) The SRA domain of UHRF1 flips 5-methylcytosine out of the DNA helix. *Nature* 455:826–829.
20. Qian C, et al. (2008) Structure and hemimethylated CpG binding of the SRA domain from human UHRF1. *J Biol Chem* 283:34490–34494.
21. Nady N, et al. (2011) Recognition of multivalent histone states associated with heterochromatin by UHRF1 protein. *J Biol Chem* 286:24300–24311.
22. Lallous N, et al. (2011) The PHD finger of human UHRF1 reveals a new subgroup of unmethylated histone H3 tail readers. *PLoS One* 6:e27599.
23. Rajakumara E, et al. (2011) PHD finger recognition of unmodified histone H3R2 links UHRF1 to regulation of euchromatic gene expression. *Mol Cell* 43:275–284.
24. Rothbart SB, et al. (2013) Multivalent histone engagement by the linked tandem Tudor and PHD domains of UHRF1 is required for the epigenetic inheritance of DNA methylation. *Genes Dev* 27:1288–1298.
25. Veland N, et al. (2017) The arginine methyltransferase PRMT6 regulates DNA methylation and contributes to global DNA hypomethylation in cancer. *Cell Rep* 21:3390–3397.
26. Pichler G, et al. (2011) Cooperative DNA and histone binding by Uhrf2 links the two major repressive epigenetic pathways. *J Cell Biochem* 112:2585–2593.
27. Rothbart SB, Strahl BD (2014) Interpreting the language of histone and DNA modifications. *Biochim Biophys Acta* 1839:627–643.
28. Zhang H, et al. (2016) A cell cycle-dependent BRCA1-UHRF1 cascade regulates DNA double-strand break repair pathway choice. *Nat Commun* 7:10201.
29. Yamaguchi L, et al. (2017) Usp7-dependent histone H3 deubiquitylation regulates maintenance of DNA methylation. *Sci Rep* 7:55.
30. Vaughan RM, et al. (2018) Comparative biochemical analysis of UHRF proteins reveals molecular mechanisms that uncouple UHRF2 from DNA methylation maintenance. *Nucleic Acids Res* 46:4405–4416.
31. Dann GP, et al. (2017) ISWI chromatin remodellers sense nucleosome modifications to determine substrate preference. *Nature* 548:607–611.
32. Wilson MD, et al. (2016) The structural basis of modified nucleosome recognition by 53BP1. *Nature* 536:100–103.
33. Wang X, et al. (2017) Molecular analysis of PRC2 recruitment to DNA in chromatin and its inhibition by RNA. *Nat Struct Mol Biol* 24:1028–1038.
34. Alabert C, et al. (2014) Nascent chromatin capture proteomics determines chromatin dynamics during DNA replication and identifies unknown fork components. *Nat Cell Biol* 16:281–293.
35. Hermann A, Goyal R, Jeltsch A (2004) The Dnmt1 DNA-(cytosine-C5)-methyltransferase methylates DNA processively with high preference for hemimethylated target sites. *J Biol Chem* 279:48350–48359.
36. Pradhan S, Bacolla A, Wells RD, Roberts RJ (1999) Recombinant human DNA (cytosine-5) methyltransferase. I. Expression, purification, and comparison of de novo and maintenance methylation. *J Biol Chem* 274:33002–33010.
37. Chen H, et al. (2013) DNA damage regulates UHRF1 stability via the SCF(β-TrCP) E3 ligase. *Mol Cell Biol* 33:1139–1148.
38. Ding G, et al. (2016) Regulation of ubiquitin-like with plant homeodomain and RING finger domain 1 (UHRF1) protein stability by heat shock protein 90 chaperone machinery. *J Biol Chem* 291:20125–20135.
39. Li T, et al. (2018) Structural and mechanistic insights into UHRF1-mediated DNMT1 activation in the maintenance DNA methylation. *Nucleic Acids Res* 46:3218–3231.
40. Luger K, Rechsteiner TJ, Richmond TJ (1999) Expression and purification of recombinant histones and nucleosome reconstitution. *Methods Mol Biol* 119:1–16.
41. Chen Z, Grzybowski AT, Ruthenburg AJ (2014) Traceless semisynthesis of a set of histone 3 species bearing specific lysine methylation marks. *ChemBioChem* 15:2071–2075.